

# Level of Fimbriation Alters the Adhesion of *Escherichia coli* Bacteria to Interfaces

Ryan B. McLay,<sup>†</sup> Hang N. Nguyen,<sup>‡</sup> Yuly Andrea Jaimes-Lizcano,<sup>†</sup> Narendra K. Dewangan,<sup>†</sup> Simone Alexandrova,<sup>†</sup> Debora F. Rodrigues,<sup>‡</sup> Patrick C. Cirino,<sup>\*,†,§</sup> and Jacinta C. Conrad<sup>\*,†</sup>

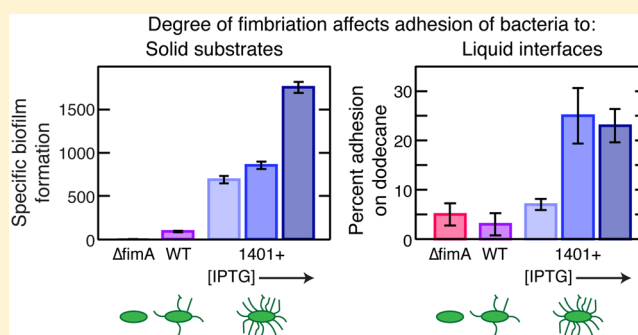
<sup>†</sup>Department of Chemical and Biomolecular Engineering, University of Houston, Houston, Texas 77204-4004, United States

<sup>‡</sup>Department of Civil and Environmental Engineering, University of Houston, Houston, Texas 77204-4003, United States

<sup>§</sup>Department of Biology and Biochemistry, University of Houston, Houston, Texas 77204-5008, United States

## Supporting Information

**ABSTRACT:** Adhesion of bacteria to interfaces is the first step in pathogenic infection, in biofilm formation, and in bioremediation of oil spills and other pollutants. Bacteria use a variety of surface structures to promote interfacial adhesion, with the level of expression of these structures varying in response to local conditions and environmental signals. Here, we investigated how overexpression of type 1 fimbriae, one such appendage, modifies the ability of *Escherichia coli* to adhere to solid substrates, via biofilm formation and yeast agglomeration, and to oil/water interfaces, via a microbial adhesion to hydrocarbon assay. A plasmid that enables inducible expression of *E. coli* MG1655 type 1 fimbriae was transformed into fimbriae-deficient mutant strain MG1655 $\Delta$ *fimA*. The level of *fimH* gene expression in the engineered strain, measured using quantitative real-time PCR, could be tuned by changing the concentration of inducer isopropyl  $\beta$ -D-1-thiogalactopyranoside (IPTG), and was higher than that in strain MG1655. Increasing the degree of fimbriation only slightly modified the surface energy and zeta potential of the bacteria, but enhanced their ability to agglomerate yeast cells and to adhere to solid substrates (as measured by biofilm formation) and to oil/water interfaces. We anticipate that the tunable extent of fimbriation accessible with this engineered strain can be used to investigate how adhesin expression modifies the ability of bacteria to adhere to interfaces and to actively self-assemble there.



## INTRODUCTION

Type 1 fimbriae are long surface nanofibers of 7 nm in width and several hundred nanometers in length. Many species of bacteria use these nanofibers to attach to rigid and soft solid surfaces as well as to liquid/air and liquid/liquid interfaces. For example, fimbriae help bacteria to attach to cells<sup>1–3</sup> and to evade antibiotics<sup>4</sup> during initial infection and hence are widely studied as a critical factor in pathogenic virulence.<sup>5</sup> Similarly, many bacteria employ type 1 fimbriae to adhere to abiotic surfaces<sup>6–11</sup> and form biofilms.<sup>12</sup> Such fimbriae-driven biofilm formation can cause deleterious biofouling;<sup>13</sup> alternately, fimbriae-driven adhesion of nonpathogenic bacteria can be used to prevent attachment by pathogenic organisms as a novel antifouling coating.<sup>14</sup> Bacterial attachment to fluid/fluid interfaces is a critical first step for bioremediation of pollutants in aqueous environments. Type 1 fimbriae help bacteria attach to liquid droplets,<sup>15–17</sup> stabilizing the liquid/liquid interface<sup>18</sup> and altering the rate at which microorganisms degrade hydrocarbons or other organic contaminants,<sup>19</sup> as well as to air/water interfaces.<sup>20</sup> Finally, type 1 fimbriae influence or generate near-surface motility behaviors—including surface approach,<sup>21</sup> “stick and roll” adhesion,<sup>22,23</sup> and mobile

adhesion<sup>24</sup>—that may affect the growth of surface-associated bacterial communities and biofilms. Hence, developing fundamental insight into bacterial adhesion, and its implications for human health and microbial technology, requires understanding how fimbriae affect the ability of bacteria to adhere to interfaces.

During attachment, micron-sized bacteria experience colloidal-scale physicochemical interactions with nearby surfaces,<sup>25–28</sup> including van der Waals, electrostatic, and Lewis acid–base interactions. Thus, theories to describe nonspecific physicochemical interactions of colloidal particles with surfaces (such as the Derjaguin–Landau–Verwey–Overbeek (DLVO)<sup>29,30</sup> or extended-DLVO (xDLVO)<sup>31,32</sup> theories) have been widely applied to predict bacterial adhesion. Although successful in some cases,<sup>33,34</sup> these models make assumptions that limit their predictive ability elsewhere.<sup>35,36</sup> The models neglect shear flow

**Special Issue:** Early Career Authors in Fundamental Colloid and Interface Science

**Received:** July 13, 2017

**Revised:** September 25, 2017

**Published:** October 4, 2017

and do not account for substrate heterogeneity found in biological or technological settings;<sup>37</sup> most crucially, they assume that bacterial surfaces are smooth and uniform—explicitly neglecting the presence of surface structures such as type 1 fimbriae. Indeed, earlier studies suggest that the adhesion of fimbriated bacteria is driven by adsorption of the fimbrial tip protein rather than by classical DLVO mechanisms.<sup>38</sup> Hence quantitative experiments to assess bacterial adhesion are essential for elucidating the controlling mechanisms in different settings. One common strategy is to generate well-controlled surfaces—including polymer brushes<sup>38–42</sup> and micro-<sup>43–45</sup> and nanotopographies<sup>46–48</sup>—for systematic studies of bacterial adhesion. Nevertheless, it remains difficult to identify biological mechanisms that influence adhesion solely by altering chemical and/or topographic properties of the substrates.

A complementary route, readily combined with substrate modification, is to engineer the bacteria themselves. The simplest strategy is to remove one or more genes of interest in a well-studied model organism such as *Escherichia coli*. Deleting one of the genes required for fimbrial expression, for example, revealed that the type 1 fimbriae of *E. coli* K12 were essential for biofilm maturation, but not initial adhesion,<sup>13</sup> and helped bacteria to resist removal by shear stresses.<sup>49</sup> Such knockout mutants provide useful insights into whether a given gene affects adhesion, but cannot be used to quantitatively probe differences in adhesion caused by changes in the level of expression. Plasmids, circular, double-stranded DNA molecules that are distinct from a given bacterium's chromosomal DNA, offer a simple means of externally tuning gene expression. Plasmid-based expression of a complete *fim* operon from a pathogenic *E. coli* strain in a different, nonvirulent *E. coli* strain whose native type 1 fimbriae are incomplete increased its adhesion to catheters, and increasing the plasmid copy number from 1 to 18 increased adhesion to catheters 10-fold.<sup>50</sup>

Here, we present an alternate and tunable approach to quantify how changes in the expression level of fimbriae modify the ability of bacteria to adhere to interfaces. The *fim* operon of *Escherichia coli* K12 strain MG1655 (wild-type) was placed under control of an inducible promoter on a medium-copy plasmid, and introduced into a *fim* deletion strain. The level of *fimH* gene expression in the engineered strain was tunable and higher than that in the parent wild-type strain, which exhibited a low level of fimbriation. Although increasing the degree of fimbriation only slightly altered the surface energy and zeta potential of the engineered bacteria, it nonetheless enhanced their ability to agglomerate yeast cells and to adhere to both solid substrates and to liquid/liquid interfaces relative to wild-type MG1655. We envision that the tunable degree of fimbriation available using this engineered bacterium will enable further quantitative physical studies relating the surface properties of bacteria to their interfacial adhesion and, more generally, to their active self-assembly during biofilm formation.

## MATERIALS AND METHODS

**Strains, Growth Conditions, and Plasmids.** Three *Escherichia coli* strains were used in this study: (i) MG1655 (wild-type); (ii) its mutant MG1655Δ*fimA* (deficient in producing fimbriae);<sup>51</sup> and (iii) MG1655Δ*fimA*+pPCC1401 (harboring plasmid pPCC1401). *E. coli* strain MC1061 was used for cloning and plasmid preparations. *Saccharomyces cerevisiae* was used in the yeast agglutination assay. Common growth and preparation media were Luria–Bertani (LB) broth (per liter: 5 g yeast extract, 5 g NaCl, 10 g Bacto-tryptone, BD Chemical); LB-agar (with 15 g agar per liter, BD Chemical); phosphate buffer solution (PBS) (per liter: 8 g NaCl, 0.2 g KCl,

1.44 g Na<sub>2</sub>HPO<sub>4</sub>, 0.24 g KH<sub>2</sub>PO<sub>4</sub>, pH adjusted to 7.4 [with HCl]); and antibiotic apramycin sulfate (50 μg mL<sup>-1</sup> stock solution, sterile filtered, Carbosynth).

Plasmid pPCC1401 is a medium copy plasmid carrying the *fim* operon (*fimA-H*) under control of a P<sub>tac</sub> promoter, such that gene expression is inducible and tunable by addition of isopropyl β-D-1-thiogalactopyranoside (IPTG). The plasmid additionally carries genes encoding the *lac* repressor (*lacI*) and apramycin resistance (*aac*). Details of plasmid construction can be found in the [Supporting Methods](#). Plasmids were introduced into cells (made electrocompetent using standard protocols) via electroporation.

**Quantitative Real-Time PCR.** The expression of *fimH* by *E. coli* MG1655Δ*fimA*+pPCC1401 was investigated using quantitative real-time PCR. Six different samples were analyzed: *E. coli* MG1655 (induced with 0.1 mM IPTG), *E. coli* MG1655Δ*fimA* (induced with 0.1 mM IPTG), and *E. coli* MG1655Δ*fimA*+pPCC1401 with different concentrations of IPTG as inducer (0.0 mM, 0.01 mM, 0.1 mM and 1.0 mM IPTG). RNA was extracted using RNeasy Mini kit (Qiagen) from cultures grown for 16 h. After RNA extraction, the DNA was cleaned up from the RNA samples with DNase I prior to synthesis of the complementary DNA (cDNA). SuperScript III reverse transcriptase (Invitrogen) was used for cDNA synthesis with random primers (Invitrogen) following the manufacturer's protocol.<sup>52</sup>

The primers for *fimH* were designed for SYBR Green master-mix using Primer Express v 2.0 (Applied Biosystems) and tested for specificity during primer optimization and sequencing as previously described.<sup>52</sup> Sequences of the forward and reverse primers (F38 and R38) are listed in Table S1 ([Supporting Methods](#)). RT-PCR was carried out with the complementary DNA (cDNA) using StepOnePlus Real-time PCR system (Applied Biosystems). The reaction contained 7.5 μL of 2× Power SYBR Green PCR master-mix (Applied Biosystems), 0.3 μL of 0.1 ng μL<sup>-1</sup> BSA, 1 μL of cDNA template, and 0.9 μL of 5 mM primer (to obtain a final primer concentration of 300 nM). The complete reaction consisted of one cycle of 95 °C for 3 min, 44 cycles at 95 °C for 15 s, and one cycle at 55 °C for 1 min. The optimization of primer concentrations was performed as described by the manufacturer of SYBR Green (Applied Biosystems). The expression of *fimH* was analyzed using the 2<sup>-ΔΔC<sub>T</sub></sup> method.<sup>53</sup> The *fimH* expression of the *E. coli* MG1655Δ*fimA*+pPCC1401 without IPTG was used as calibrator and the 16S rRNA gene was used to normalize the results.<sup>54–56</sup> The 16S rRNA reference and *fimH* target gene were validated following the 2<sup>-ΔΔC<sub>T</sub></sup> method<sup>53</sup> ([Supporting Methods](#)). All samples were prepared and run in triplicate.

**Transmission Electron Microscopy (TEM).** Type 1 fimbriae are much too small to be resolved with conventional light microscopy. Instead, TEM was used to visually confirm the presence or absence of fimbriae. Cultures for TEM experiments were grown (i) from an overnight subculture in LB or (ii) from a culture that was cleaned and resuspended in HEPES buffer (fixed in 0.1% glutaraldehyde solution). For (i), 1 day prior to imaging the cells were grown overnight from a subculture and grown to the late exponential phase, then cleaned and resuspended in 10 mM HEPES buffer. Approximately 12 h before imaging, the washed cells were resuspended in a 0.1% glutaraldehyde solution to fix them. For (ii), cells were grown in LB (from a subculture) with fimbriation induced by addition of 1.0 mM IPTG and diluted to an optical density (OD, measured at a wavelength λ = 595 nm on a NOVostar plate reader (BMG Labtech) of 0.5 the morning of imaging. There was no noticeable difference in the quality of images obtained using these methods.

After cell preparation but prior to grid incubation, two 20 μL drops of DI water and two 20 μL drops of uranyl acetate (a TEM stain that interacts with lipids and proteins to enhance contrast) were deposited onto Parafilm. Next, 2–5 μL of a bacterial suspension was pipetted onto a freshly glow-discharged carbon-coated TEM grid and allowed to rest for 30–90 s. Subsequently, the cell-adsorbed grid was washed twice: transferred using forceps into a small 20 μL drop of DI water on wax paper and rapidly dried by wicking away excess water. After washing, the grid was quickly (~1 s) deposited into a 20 μL drop of 2% (w/v) uranyl acetate and then blotted dry; the uranyl acetate staining was repeated with a longer staining time (~15 s) and wicked

dry. Finally, grids were dried in air. Prepared grids were observed in a JEOL 1200 EX TEM operated at an acceleration voltage of 100 kV and electron micrographs were recorded using a 2k slow-scan CCD camera (model 14C, SIA) at a user-defined magnification.

**Yeast Agglutination Assay (YAA).** A modified yeast agglutination assay<sup>57</sup> was developed to semiquantitatively assess the degree of fimbriation of the bacteria. Two methods were used to prepare yeast cultures. In the first, pellets of *S. cerevisiae* were mixed in phosphate buffer solution (PBS) at a concentration of 5 mg mL<sup>-1</sup>; in the second, yeast pellets were grown overnight in LB medium (37 °C, with shaking) and then centrifuged and washed twice with PBS. (The method of yeast preparation did not affect the assay results.) Following growth, the yeast suspension was then diluted to an OD of 8.0. Bacterial strains were inoculated from an overnight subculture starting at an OD of 0.05 and grown statically in LB ± apramycin to an OD of 0.7. Next, cultures were induced with various concentrations of IPTG and then grown to late exponential phase. Finally, the bacterial cultures were twice centrifuged at 4000 g for 15 min and resuspended in PBS, and then diluted to an OD of 1.0.

For the assay, 500 μL of each suspension (yeast and bacteria) was transferred into a single centrifuge tube. Where noted, methyl α-D-mannopyranoside (Sigma-Aldrich) (a nonmetabolizable analogue of mannose, known to bind the FimH adhesin on the tip of type 1 fimbriae)<sup>58</sup> was added at a final concentration of 100 mM to bacterial suspensions to fully occupy the mannose-binding fimbrial tips 5 min before adding the yeast suspension. After mixing, the cells were left to react quiescently for 3–5 h, after which each centrifuge tube was vortexed at ~2200 rpm for 10 s. In the absence of bacteria, yeast remained suspended in solution over 30 min and the solution remained turbid (Figure S1). Bacteria that bound to yeast cells formed large aggregates that sedimented out of solution and deposited on the bottom of the centrifuge tubes over time, such that the turbidity of the remaining solution depended on the time since vortexing. Hence, the turbidity was measured for each sample at 0, 3, 5, 10, 20, and 30 min after vortexing. For turbidity measurements, a 20 μL aliquot was carefully taken from the center of the centrifuge tube at the same depth for each measurement. The removed aliquot was diluted 10-fold in PBS and turbidity/absorbance was measured in a 96-well plate. Each experiment was repeated at least three times. For the noninducible strains, we confirmed that the presence or absence of IPTG did not affect the change in absorbance over time (as shown for representative data in Figure S2).

**Surface Characterization via Zeta Potential and Surface Energy.** For ζ-potential measurements, *E. coli* bacteria were grown in LB medium for 21 h (with or without IPTG present during growth), washed twice in DI water at 5000 rpm for 10 min, and finally resuspended in DI water. Prior to ζ-potential measurements, each suspension was diluted to an OD of 0.04 with DI water. Zeta potentials were measured using a Nicomp 380ZLSn particle sizer ζ-potential analyzer. Bacterial lawns were then prepared on cellulose acetate membrane filters (pore diameter 0.45 μm, Advantec) by negative pressure filtration of a bacterial suspension. Filters with bacterial lawns were glued to a thin layer of dental wax (Electron Microscopy Sciences) just above its melting point on a glass slide. Next, static contact angles for deionized water, diiodomethane (99%, Sigma), and ethylene glycol (99%, Sigma) on the cell lawns were measured using a Dataphysics OCA 15EC goniometer. The surface energy was calculated using algorithms built into the instrument's analysis package, which were based on the method of Wu.<sup>59</sup>

**Specific Biofilm Formation (SBF) Assay.** Specific biofilm formation measures the growth of biofilms over time, relative to the growth rate of the bacteria. The effect of fimbriation on the growth of bacterial biofilms on solid surfaces over time was assessed via a SBF assay,<sup>60,61</sup> using bacterial cultures inoculated into sterile 96-well plates. Bacterial cultures were grown overnight from a fresh colony and subcultured the following morning (starting at an OD of 0.05) and allowed to grow to midexponential phase. This suspension was then diluted to an OD of 0.2 immediately prior to the start of the SBF assay. Aliquots of 300 μL of cell culture were injected into wells of a sterile 96-well plate and covered with sterile aluminum foil; the 96-well plate

and aluminum covers were sterilized via concurrent soaking in ethanol and irradiation with UV for 1 h. The 96-well plate was then statically incubated at 30 °C for 12, 24, or 48 h. Following incubation, aliquots of liquid cultures were diluted 10:1 in LB media and the ODs of the diluted liquid cultures were measured (to quantify relative cell growth). Any solution remaining in the wells was decanted. Each well was washed three times in 300 μL of PBS to remove cells that were not bound to the wells; subsequently, the remaining cells were stained by adding crystal violet (CV, 300 μL of a 0.1% w/v mixture) in DI water for 20 min. After incubation, the CV stain was removed and the wells were again washed three times in PBS, after which 300 μL of an acetone/ethanol mixture (20:80, v/v) was added to release the bound cells from the surface of the wells. Finally, the OD of the eluted CV-stained biofilm was then measured to quantify the level of biofilm development.<sup>62</sup> Each assay was repeated for 12 replicates from two separate cultures. These values were then averaged to calculate the specific biofilm formation (SBF) as

$$\text{SBF} = \frac{(B - NC)}{G} \times 100 \quad (1)$$

where *B* is the optical density of the eluted CV-stained biofilm (i.e., the amount of CV-stained biofilm formed), *NC* is the amount of CV that adhered to the 96-well plates in the absence of cells (i.e., the absorbance of the CV-stained growth medium), and *G* is the OD of cells grown in each suspended culture.

**Microbial Adhesion to Hydrocarbons (MATH) assay.** A MATH assay<sup>63</sup> was used to assess adhesion to liquid/liquid interfaces. In this assay, the absorbance of an aqueous cell suspension and a hydrophobic phase are measured before and after mixing to determine the concentration of cells that partition into the hydrophobic phase. Bacterial cultures were grown to a desired OD (corresponding to late exponential phase); centrifuged at 5000 rpm and washed with 15 mL of PBS twice to remove all carbon sources; and finally diluted to an OD of 1.0. For the assay, 4 mL of the cell suspension and 1 mL of hydrocarbon (*n*-dodecane or hexadecane) were sequentially transferred into a 15 mL centrifuge tube. Each solution, containing cells and hydrocarbons, was vigorously vortexed at ~3200 rpm for 120 s and then allowed to phase separate into two distinct liquid phases for at least 40 min. After phase separation, the OD of the bottom aqueous layer was measured with care to avoid transferring additional hydrocarbon into the spectrophotometer cuvette. Each measurement was repeated at least three times on at least two independent cultures. We report the percent adhesion of the cells, defined as

$$\text{Percent adhesion} = \left[ 1 - \frac{\text{OD}_{600}(\text{before vortexing})}{\text{OD}_{600}(\text{after vortexing})} \right] \times 100 \quad (2)$$

## RESULTS AND DISCUSSION

**Tunable Expression of a Fimbrial Gene.** We first confirmed that the engineered *E. coli* strain exhibited tunable levels of *fim* operon expression using quantitative PCR. Briefly, we measured the fold change in expression of *fimH* for different strains (at a fixed IPTG concentration of 0.1 mM) and for different concentrations of IPTG (for the engineered strain). For each strain, the change in expression was measured relative to that of a reference gene to correct for variations arising in the sample preparation and in the PCR cycling process (Note: The 16S rRNA gene used here is commonly chosen as a reference gene in microbiology, because its expression level remains approximately constant across different strains and under different conditions). The relative level of gene expression increased with the concentration of (nonmetabolizable) inducer IPTG, as shown in Figure 1. Compared to the uninduced MG1655Δ*fimA*+pPCC1401 strain, the expression level of *fimH* was 4, 14, and 22 times higher upon adding IPTG

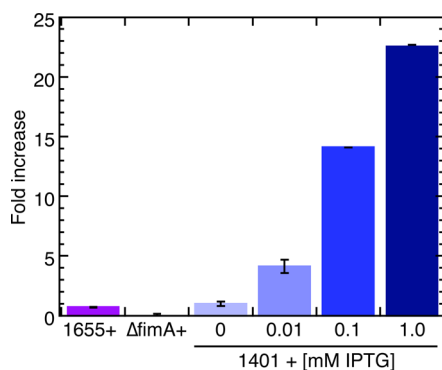


**Figure 1.** Control over fimbriation in the engineered inducible strain MG1655 $\Delta fimA$ +pPCC1401. Fold increase over the expression level of *fimH* in uninduced MG1655 $\Delta fimA$ +pPCC1401 for (left to right): MG1655 (wild type) + 0.1 mM IPTG; MG1655 $\Delta fimA$  (isogenic deletion mutant) + 0.1 mM IPTG; MG1655 $\Delta fimA$ +pPCC1401 (engineered strain) + 0 mM IPTG; MG1655 $\Delta fimA$ +pPCC1401 + 0.01 mM IPTG; MG1655 $\Delta fimA$ +pPCC1401 + 0.1 mM IPTG; MG1655 $\Delta fimA$ +pPCC1401 + 1.0 mM IPTG. Gene expression of *fimH* was measured using quantitative real-time PCR by the  $2^{-\Delta\Delta C_T}$  method.<sup>53</sup> Error bars indicate the 95% confidence intervals, calculated from the standard deviation over three independent replicates.

at concentrations of 0.01, 0.1, and 1.0 mM, respectively. Wild-type strain MG1655 exhibited slightly lower expression levels of *fimH* than the engineered but uninduced MG1655 $\Delta fimA$ +pPCC1401 strain, owing to leaky expression from the *Ptac* promoter. The deletion mutant MG1655 $\Delta fimA$  showed nearly no expression of *fimH*. Hence we concluded that the engineered *E. coli* exhibited inducible and tunable *fim* gene expression, required to produce adhesive type 1 fimbriae.

**Surface Characterizations of Bacteria.** To confirm that induced cells indeed produced fimbriae, we imaged selected bacteria using transmission electron microscopy. TEM images revealed differences in the number of fimbriae on wild-type MG1655, deletion mutant MG1655 $\Delta fimA$ , and induced MG1655 $\Delta fimA$ +pPCC1401 bacteria, as shown in Figure 2. Wild-type bacteria exhibited only very few fimbriae (Figure 2a and its inset) and the MG1655 $\Delta fimA$  deletion mutant had no fimbriae (Figure 2b). Induction of the pPCC1401 plasmid by addition of a high concentration of IPTG, however, led to marked fimbrial expression (Figure 2c). These results are consistent with the qPCR measurements in Figure 1.

Although the TEM images revealed the presence or absence of nanoscale appendages on the surface of bacteria, variation in sample handling and in the density of fimbriae in the images precluded quantitative comparison of the extent of fimbriation. Furthermore, we seek to understand how the extent of fimbriation influences the extent to which *E. coli* binds FimH substrates (mannosides), such as those on the yeast surface. Hence, we developed a simple, rapid, and semiquantitative modified yeast agglutination assay (YAA). *E. coli* expressing fimbriae readily agglutinate yeast and red blood cells<sup>57</sup> to form large aggregates, which sediment out of the solution. We therefore postulated that the relative degree of fimbriation could be assessed via the rate of sedimentation of the aggregates. For low  $Re < 0.1$ , the settling velocity of a microscale particle scales with the square of its diameter:  $v_s = g(\rho_p - \rho)D_p^2/18\mu$ , where  $g$  is the gravitational acceleration constant,  $\rho_p$  is the density of the settling particles (1.087 g mL<sup>-1</sup>),  $\rho$  is the density of the medium in which the particles are suspended (0.998 g mL<sup>-1</sup>),  $D_p$  is the diameter of the settling particle, and  $\mu$  is the viscosity of the fluid medium (1.0 cP). In the modified YAA, we expected that increasing the number of fimbriae on the bacteria would increase the size of the aggregates<sup>57</sup> and in turn lead to faster sedimentation.

To assess the rate of sedimentation, we monitored the change over time of the absorbance of suspensions containing *E. coli* and yeast that were allowed to bind for 3–5 h and then rapidly vortexed to resuspend any aggregates. Pronounced differences in the rate of change of the absorbance over 30 min were correlated with the presence or absence of fimbriae on *E. coli* that were available to bind yeast, as shown in Figure 3. The absorbance of samples containing the induced engineered strain MG1655 $\Delta fimA$ +pPCC1401 rapidly decreased over time, consistent with sedimentation of large aggregates containing bacteria and yeast. As the concentration of IPTG was increased, the rate of change of the absorbance of the solution increased slightly, as seen by comparing the data at 3 min and at 5 min (before the aggregates had completely settled out); the 95% confidence intervals for bacteria induced with IPTG concentrations of 0.01 mM and 1.0 mM do not overlap. This comparison suggests that increased fimbriation led to slightly larger bacteria-yeast aggregates. In sharp contrast, the absorbance of samples containing fimbriae-deficient bacteria, such as the noninduced MG1655 $\Delta fimA$ +pPCC1401 or MG1655 $\Delta fimA$ , decreased only slightly over 30 min, suggesting that bacteria and yeast remained dispersed in

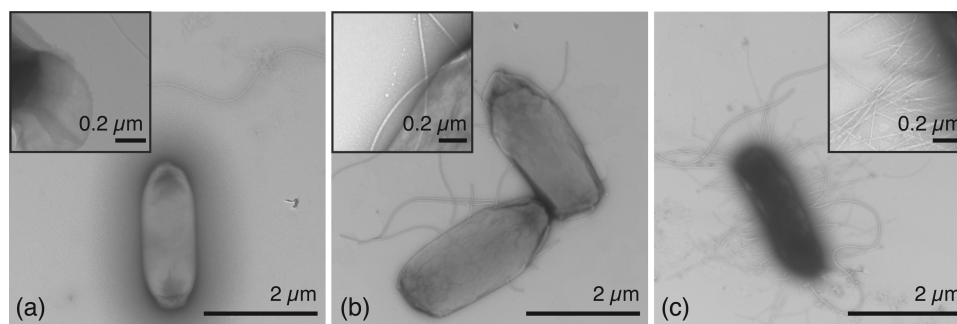


**Figure 2.** Representative transmission electron micrographs of (a) the wild-type MG1655 strain, (b) the fimbrial deletion mutant MG1655 $\Delta fimA$ , and (c) the induced engineered MG1655 $\Delta fimA$ +pPCC1401 strain. Type 1 fimbriae appear as slender faint nanofibers. The inset to (a) shows that the wild-type strain expresses very few fimbriae under these culture conditions; the inset to (c) provides a magnified image of the fimbriae on the induced engineered strain. All strains were grown in the presence of 1.0 mM IPTG. The longer and wider filamentous appendages visible in all images are flagella.

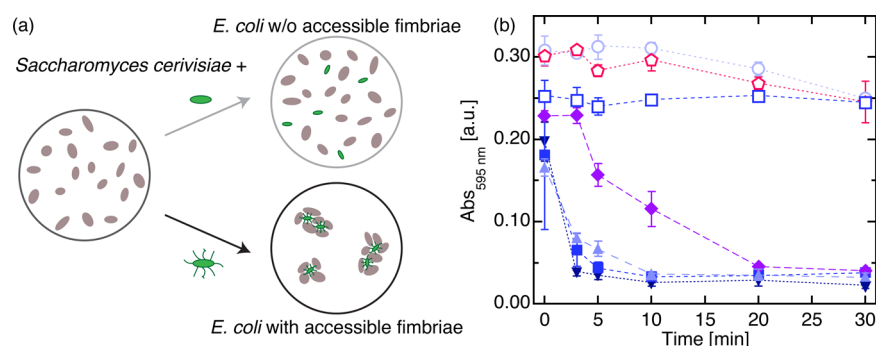


**Figure 3.** Modified yeast agglutination assay reveals differences in the degree of fimbriation. (a) Schematic of the yeast agglutination assay: *S. cerevisiae* yeast were added to a suspension containing *E. coli* bacteria. If the bacteria bore accessible fimbriae, they bound to the yeast to form large aggregates, which rapidly sedimented out of suspension; if they did not bear accessible fimbriae, they remained dispersed. (b) Solution absorbance at 595 nm,  $Abs_{595\text{ nm}}$ , as a function of time after vortexing. Symbols: (◆) MG1655 (wild type); (◇) MG1655 $\Delta$ *fimA* (isogenic deletion mutant); (○) MG1655 $\Delta$ *fimA*+pPCC1401 (engineered strain); (■) MG1655 $\Delta$ *fimA*+pPCC1401 + 0.01 mM IPTG; (▀) MG1655 $\Delta$ *fimA*+pPCC1401 + 0.1 mM IPTG; (▼) MG1655 $\Delta$ *fimA*+pPCC1401+1.0 mM IPTG; (□) MG1655 $\Delta$ *fimA*+pPCC1401 + 0.1 mM IPTG + methyl- $\alpha$ -D-pyranoside. Error bars indicate the 95% confidence intervals, calculated from the standard deviation over three independent replicates.

solution. These bacteria lacked the fimbriae required to bind to yeast and hence did not form aggregates. Similarly, when excess methyl- $\alpha$ -D-mannopyranoside (Mann(Pyr), a nonmetabolizable analogue of mannose) was present during the resting period, the FimH binding domain of fimbriae bound to Mann(Pyr). Fimbriae fully occupied by Mann(Pyr) were unable to bind to the yeast cells, so that yeast and bacteria remained dispersed in solution and did not sediment out over 30 min, as in the nonfimbriated and uninduced strains. The rate of sedimentation for MG1655 was between that of the nonfimbriated strains and the induced hyperfimbriated strains, suggesting an intermediate (low) degree of fimbriation consistent with the TEM images presented in Figure 2.

**Surface Energy and Zeta Potential.** Next, we assessed the change imparted by differences in the degree of fimbriation on the average surface properties of the bacteria via  $\zeta$ -potential and surface energy measurements. The zeta potential of the wild-type MG1655 strain,  $-42$  mV, was unchanged whether the bacteria were grown in the presence or absence of IPTG, as shown in Table 1. Deleting the *fimA* gene did not alter the zeta potential. In the absence of IPTG, the zeta potential of the engineered MG1655 $\Delta$ *fimA*+pPCC1401 strain equaled that of the wild-type and knockout mutants. Upon addition of IPTG, the magnitude of the zeta potential decreased by  $\sim 17\%$  (from  $-42$  mV for the wild-type in the absence of IPTG to  $-35$  mV

**Table 1. Surface Energy and Zeta Potential of Strains Grown in the Presence or Absence of the Inducing Agent IPTG<sup>a</sup>**

strain	[IPTG] (mM)	zeta potential (mV)	surface energy (mN m)
MG1655 (wild-type)	0	$-42 \pm 1$	60.1
	0.1	$-41 \pm 2$	$61.5 \pm 0.1$
MG1655 $\Delta$ <i>fimA</i>	0	$-41 \pm 1$	66.8
	0.1	$-43 \pm 1$	60.5
MG1655 $\Delta$ <i>fimA</i> +pPCC1401	0	$-40 \pm 2$	57.1
	0.01	$-36 \pm 2$	56.2
	0.1	$-36 \pm 1$	$43.2 \pm 0.5$
	1.0	$-35 \pm 1$	$60.5 \pm 3.2$

<sup>a</sup>Error bars correspond to the standard deviation over five replicate measurements. The standard deviation for the surface energy (where indicated) was calculated from data obtained for two bacterial lawns prepared with different bacteria cultures.

for the engineered strain at the greatest IPTG concentration). The electrostatic DLVO repulsion scales approximately as the square of the zeta potential, and hence the repulsive barrier would be expected to decrease by  $\sim 30\%$  across our experimental conditions. This decrease is likely not significant, given that adhesion of *E. coli* to glass substrates is determined by a complicated interplay of electrostatic, steric, hydrophobic, and van der Waals interactions.<sup>64</sup> The surface energy of bacterial lawns, grown in the presence or absence of IPTG, varied somewhat from strain to strain but did not correlate with IPTG concentration or fimbrial expression. We therefore concluded that changes in fimbriation did not systematically affect the colloidal-scale physicochemical properties of the bacteria.

**Effects of Fimbriae on Interfacial Adhesion.** We first quantified the ability of bacteria to adhere to and form biofilms on solid substrates via a Specific Biofilm Formation (SBF)<sup>60</sup> assay. In this assay, bacteria were grown in 96-well plates for a fixed time interval, stained with crystal violet, and then released from the well surface using a mixture of acetone and ethanol. From the absorbance of the solution containing the eluted biofilms we calculated the SBF, standardized to abiotic control wells that contained only the LB growth medium, using eq 1. Higher values of SBF indicated higher rates of biofilm growth (relative to cell growth rate). The induced engineered strain exhibited dramatically greater levels of biofilm growth than either the wild-type or the knockout mutant, as shown in Figure 4. Increasing the concentration of IPTG increased the amount of biofilm formed: the 5.5-fold change in expression of FimH upon increasing the IPTG concentration 100-fold from 0.01 to 1.0 mM (cf. Figure 1) led to a 3.5-fold increase (at 6 h growth) or 2.5-fold (at 12 h growth) increase in SBF. This increase did not occur uniformly across the tested range of IPTG and was more pronounced at higher IPTG concentrations. By contrast, the deletion mutant (which did not express fimbriae) showed almost no biofilm formation and the wild-type strain (which bore few fimbriae) had similarly low biofilm formation. To determine whether fimbriae affected the initial attachment as well as biofilm growth, we measured the rate at which bacteria were deposited onto a hydrophobic substrate from flow.<sup>65</sup> The rate at which hyperfimbriated bacteria (MG1655 $\Delta$ *fimA*+pPCC1401 + 0.1 mM IPTG) deposited,  $5 \text{ cell min}^{-1}$ , was greater than that at which fimbriae-deficient MG1655 $\Delta$ *fimA* or

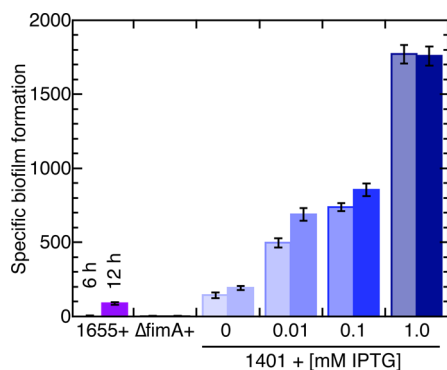


**Figure 4.** Specific biofilm formation (SBF, expressed as a percentage of the control) for *E. coli* over (left, light) 6 h and (right, dark) 12 h. From left to right: MG1655 (wild type) + 0.1 mM IPTG; MG1655 $\Delta$ fimA (isogenic deletion mutant) + 0.1 mM IPTG; MG1655 $\Delta$ fimA+pPCC1401 (engineered strain) + 0 mM IPTG; MG1655 $\Delta$ fimA+pPCC1401 + 0.01 mM IPTG; MG1655 $\Delta$ fimA+pPCC1401 + 0.1 mM IPTG; MG1655 $\Delta$ fimA+pPCC1401 + 1.0 mM IPTG. Error bars represent the 95% confidence intervals, calculated from the standard deviation across 12 measurements on two independent cultures.

wild-type MG1655 bacteria deposited ( $\sim 1$  cell  $\text{min}^{-1}$ , Figure S3). These results are consistent with earlier studies showing that type 1 fimbriae aid in attachment to solid surfaces<sup>50</sup> (as hyperfimbriation increased the rate at which the bacteria deposited) and in biofilm maturation thereon<sup>13</sup> (as the highly fimbriated strains had increasingly higher SBF values and the nonfimbriated strain had a near-zero SBF).

Second, we examined the ability of bacteria to adhere to liquid–liquid interfaces, relevant for bioremediation of pollutants in aqueous environments, using a microbial adhesion to hydrocarbons (MATH) assay. The classic MATH assay is thought to measure the hydrophobicity of cells, but this interpretation is complicated by interfacial interactions between the hydrocarbon and aqueous phases.<sup>66</sup> Here, we use the MATH assay to semiquantitatively assess adhesion to oil–water interfaces,<sup>16,17</sup> relevant for biodegradation<sup>19</sup> and for biofilm growth.<sup>67,68</sup> The FimH adhesin is a two-domain system, in which a pilin domain connects a lectin domain to the major fimbrial subunit (*FimA*) with a mannose-binding pocket located at the lectin tip. Because the binding pocket is lined with hydrophobic tyrosine AA residues, we hypothesized that *E. coli* expressing a larger number of fimbriae would exhibit greater adhesion to the interface between water and a hydrocarbon phase.<sup>69</sup>

Bacteria suspended in an aqueous phase were thoroughly mixed with an immiscible alkane often found in crude oil, either dodecane (C-12) or hexadecane (C-16). Their relative abundance depends on the source of oil; NIST Standard Reference Material (2779), as one example, contains about 10% *n*-alkanes and dodecane is in greater abundance than hexadecane,<sup>70</sup> whereas the hexadecane is more abundant than dodecane in crude oil from Pennsylvania and Ohio.<sup>71</sup> After mixing, the two phases were allowed to separate under gravity for at least 40 min. From the turbidity of the aqueous phase (corresponding to the fraction of cells that partitioned therein), we estimated the percentage of cells adhering to the hydrocarbon via eq 2. For IPTG concentrations greater than or equal to 0.1 mM, the induced engineered MG1655 $\Delta$ fimA + pPCC1401 strain adhered significantly more to the hydrocarbon phase than either the uninduced strain or the

nonengineered wild-type MG1655 (as determined from the 95% confidence intervals), as shown in Figure 5. At the lowest

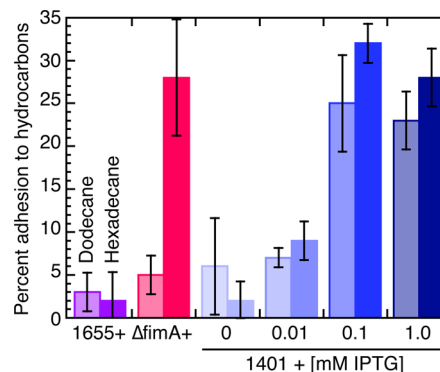


**Figure 5.** Percent adhesion to a dispersed hydrocarbon phase of the induced versus uninduced *E. coli* strains, measured via a MATH assay on (left, light) dodecane or (right, dark) hexadecane. From left to right: MG1655 (wild type) + 0.1 mM IPTG; MG1655 $\Delta$ fimA (isogenic deletion mutant) + 0.1 mM IPTG; MG1655 $\Delta$ fimA+pPCC1401 (engineered strain) + 0 mM IPTG; MG1655 $\Delta$ fimA+pPCC1401 + 0.01 mM IPTG; MG1655 $\Delta$ fimA+pPCC1401 + 0.1 mM IPTG; MG1655 $\Delta$ fimA+pPCC1401 + 1.0 mM IPTG. Error bars represent the 95% confidence intervals, calculated from the standard deviation across two or three independent cultures.

IPTG concentration of 0.01, the adhesion of MG1655 $\Delta$ fimA + pPCC1401 was only slightly larger than that of the wild-type and was not statistically different from that of the uninduced strain. These results were qualitatively confirmed by directly imaging bacteria near the oil/water interface using confocal microscopy (data not shown). Similar results were obtained for the two different alkanes for the wild-type and for MG1655 $\Delta$ fimA + pPCC1401 for all concentrations of IPTG (explicitly, the mean values of the percentage adhesion were not distinct per the 95% confidence intervals). As wild-type *E. coli* typically exhibits minimal adhesion to hydrocarbons,<sup>13</sup> the results presented in Figure 5 suggest that fimbriation can enhance adhesion to liquid–liquid interfaces, as has been observed for other bacterial species on oil–water interfaces.<sup>15</sup> This result is also consistent with an earlier study that indicated that fimbriated *E. coli* strains are more hydrophobic than nonfimbriated strains.<sup>72</sup>

The adhesion of the fimbrial deletion mutant MG1655 $\Delta$ fimA, however, depended on the choice of hydrocarbon. Somewhat surprisingly, low adhesion was observed on dodecane, but very high adhesion was observed on hexadecane. This finding suggests that other bacterial surface structures, exposed or produced when type 1 fimbriae are absent,<sup>49</sup> may contribute differently to adhesion on liquids of varying hydrophobicity. Surface structures that are known to contribute to cell-surface hydrophobicity for *E. coli* include outer membrane proteins,<sup>73</sup> oligosaccharides,<sup>74</sup> lipopolysaccharides,<sup>75</sup> and p-fimbriae;<sup>76</sup> in addition, flagella can also increase surface adhesion. More detailed surface characterization and/or differential gene expression studies may provide insights into the surprising (and noteworthy) adhesion of MG1655 $\Delta$ fimA to hexadecane.

**Dependence of Adhesion Metrics on Inducer Concentration.** Interestingly, adhesion to the liquid/liquid interface (assessed via the MATH assay) exhibited a functional dependence on IPTG concentration that was distinct from that

of the SBF. The percent adhesion to hydrocarbons exhibited a step change: for  $[IPTG] = 0.01$  mM, it was only slightly larger than the value for the wild-type strain; for  $[IPTG] \geq 0.1$  mM, it was approximately concentration-independent. By contrast, the SBF increased monotonically (but not uniformly) with increasing IPTG. To highlight the difference in adhesion to a liquid–liquid interface on IPTG concentration, we therefore examined the  $[IPTG]$ -dependence of the quantitative metrics from Figures 1, 3, 4, and 5. To uniformly compare across metrics that increase with IPTG concentration, we chose as the YAA metric the inverse of the absorbance at 3 min. For adhesion to solid surfaces, we chose the values of the SBF at 6 h and at 12 h; for adhesion to liquid interfaces (MATH assay), we chose the percent adhesion to dodecane and to hexadecane. The fold-increase in expression of *FimH*, obtained from the qPCR experiment, increased approximately as the logarithm of  $[IPTG]$  (Figure 6a). None of the three adhesion metrics, however, exhibited this logarithmic dependence on  $[IPTG]$ . Both metrics assessing adhesion to solid surfaces (biotic, via inverse absorbance, Figure 6b, and abiotic, the SBF, Figure 6c) increased more rapidly at high IPTG concentrations; by contrast, the liquid adhesion metric (percent adhesion to hydrocarbons, Figure 6d) increased rapidly at low  $[IPTG]$  but

was approximately independent of  $[IPTG]$  between 0.1 and 1.0 mM. The different functional dependence of these metrics suggests that fimbriae differently interact with and mediate adhesion to solid and to liquid interfaces.

## CONCLUSIONS

We showed that controlling the level of fimbriation using an inducible plasmid altered the ability of *E. coli* bacteria to adhere to liquid–solid and liquid–liquid interfaces. The dependence of adhesion on the degree of fimbriation, probed through simple bulk assays, differed for the two types of interfaces. We anticipate that this engineered strain can be used as a tunable model system for detailed and systematic physical measurements probing the effects of adhesin expression to biofilm formation on solid<sup>50</sup> and liquid<sup>68,77</sup> interfaces. Moreover, with increasing interest in technological applications of biofilms, tunable control over fimbriation may prove useful for tailoring, e.g., the interfacial and/or mechanical properties of antifouling coatings composed of benign bacteria<sup>14</sup> or of biofilms to remove toxic metals from polluted water.<sup>78,79</sup>

This study reports changes in the average propensity of bacteria to adhere to interfaces that are correlated with the average degree of fimbriation. Nonetheless, even genetically identical bacteria can exhibit cell-to-cell phenotypic variability,<sup>80</sup> so that the averages may mask what may be pronounced cell-to-cell variation. We thus expect that our tunably fimbriated strain may be used with advanced techniques to assess the properties of individual cells and thereby generate further insight into the connection between fimbriation and adhesion: for example, by monitoring the dynamics of bacterial approach and adhesion at the single-cell scale via total internal reflectance fluorescence microscopy<sup>49,81,82</sup> or digital holographic microscopy,<sup>83,84</sup> and by measuring the forces exerted by single cells using AFM.<sup>64,85</sup>

## ASSOCIATED CONTENT

### Supporting Information

The Supporting Information is available free of charge on the ACS Publications website at DOI: 10.1021/acs.langmuir.7b02447.

Three figures, two tables, and Supporting Methods: Figure S1 (Absorbance of a solution of *S. cerevisiae* yeast over 30 min); Figure S2 (Comparison of yeast agglutination assay results for MG1655 bacteria with and without IPTG); Figure S3 (Number of bacteria deposited on a surface from flow as a function of time); Table S1 (Primers used in this study); Table S2 (Contact angle and surface energy calculations); Supporting Methods (description of plasmid construction, calibration and normalization of the RT-qPCR data via the  $2^{-\Delta\Delta C_T}$  method, contact angle measurements, and deposition assay) (PDF)

## AUTHOR INFORMATION

### Corresponding Authors

\*E-mail: pccirino@uh.edu.

\*E-mail: jconrad@uh.edu.

### ORCID

Debora F. Rodrigues: 0000-0002-3124-1443

Jacinta C. Conrad: 0000-0001-6084-4772

### Notes

The authors declare no competing financial interest.

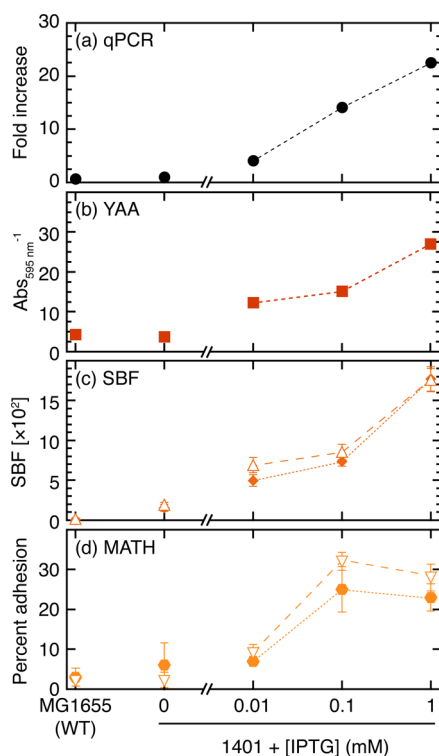


**Figure 6.** Comparison of the different assays used to assess fimbriation in the engineered strain MG1655 $\Delta$ *fimA*+pPCC1401 as a function of the inducer concentration. (a) Fold increase over the expression level of *fimH* relative to uninduced MG1655 $\Delta$ *fimA*+pPCC1401 (from Figure 1). (b) Inverse of the absorbance at 595 nm at a time of 3 min (from Figure 3). (c) Specific biofilm formation at 6 h (◆) and 12 h (△) (from Figure 4). (d) Percent adhesion to dodecane (●) and hexadecane (▽) (from Figure 5). Data for the wild-type MG1655 strain + 0.1 mM IPTG are shown for comparison. Error bars represent the 95% confidence intervals for each measurement; for (a), (c), and (d), they are obtained as indicated in the parent figures, and for (b) they are propagated from the errors from the parent figure. Error bars in (a) and (b) are smaller than the symbol sizes.

## ACKNOWLEDGMENTS

This research was made possible in part by a grant from The Gulf of Mexico Research Initiative, and in part by the National Science Foundation (DMR-1151133 to JCC, CBET-1511425 to PCC, and CBET-1150255 to DFR) and the Welch Foundation (E-1869 to JCC). Data are publicly available through the Gulf of Mexico Research Initiative Information & Data Cooperative (GRIIDC) at <https://data.gulfresearchinitiative.org> (doi:10.7266/N73F4N1N.).

## REFERENCES

- (1) Abraham, S. N.; Sun, D.; Dale, J. B.; Beachey, E. H. Conservation of the D-Mannose-Adhesion Protein Among Type 1 Fimbriated Members of the Family Enterobacteriaceae. *Nature* **1988**, *336*, 682–684.
- (2) Zhou, G.; Mo, W.-J.; Sebbel, P.; Min, G.; Neubert, T. A.; Glockshuber, R.; Wu, X.-R.; Sun, T.-T.; Kong, X.-P. Uroplakin Ia is the Urothelial Receptor for Uropathogenic *Escherichia coli*: Evidence from In Vitro FimH Binding. *J. Cell Sci.* **2001**, *114*, 4095–4103.
- (3) Duncan, M. J.; Li, G.; Shin, J.-S.; Carson, J. L.; Abraham, S. N. Bacterial Penetration of Bladder Epithelium through Lipid Rafts. *J. Biol. Chem.* **2004**, *279*, 18944–18951.
- (4) Vizcarra, I. A.; Hosseini, V.; Kollmannsberger, P.; Meier, S.; Weber, S. S.; Arnoldini, M.; Ackermann, M.; Vogel, V. How Type 1 Fimbriae Help *Escherichia coli* to Evade Extracellular Antibiotics. *Sci. Rep.* **2016**, *6*, 18109.
- (5) Connell, I.; Agace, W.; Klemm, P.; Schembri, M.; Mårild, S.; Swanborg, C. Type 1 Fimbrial Expression Enhances *Escherichia coli* Virulence for the Urinary Tract. *Proc. Natl. Acad. Sci. U. S. A.* **1996**, *93*, 9827–9832.
- (6) Otto, K.; Norbeck, J.; Larsson, T.; Karlsson, K.-A.; Hermansson, M. Adhesion of Type 1-Fimbriated *Escherichia coli* to Abiotic Surfaces Leads to Altered Composition of Outer Membrane Proteins. *J. Bacteriol.* **2001**, *183*, 2445–2453.
- (7) Cookson, A. L.; Cooley, W. A.; Woodward, M. J. The Role of Type 1 and Curli Fimbriae of Shiga Toxin-Producing *Escherichia coli* in Adherence to Abiotic Surfaces. *Int. J. Med. Microbiol.* **2002**, *292*, 195–205.
- (8) Kalivoda, E. J.; Stella, N. A.; O'Dee, D. M.; Nau, G. J.; Shanks, R. M. Q. The Cyclic AMP-Dependent Catabolite Repression System of *Serratia marcescens* Mediates Biofilm Formation through Regulation of Type 1 Fimbriae. *Appl. Environ. Microbiol.* **2008**, *74*, 3461–3470.
- (9) Chao, Y.; Zhang, T. Probing Roles of Lipopolysaccharide, Type 1 Fimbria, and Colanic Acid in the Attachment of *Escherichia coli* Strains on Inert Surfaces. *Langmuir* **2011**, *27*, 11545–11553.
- (10) Mhedbi-Hajri, N.; Jacques, M.-A.; Koebnik, R. Adhesion Mechanisms of Plant-Pathogenic Xanthomonadaceae. In *Bacterial Adhesion: Chemistry, Biology and Physics*, Linke, D.; Goldman, A., Eds.; Springer: Dordrecht, 2011; pp 71–89.
- (11) Murphy, C. N.; Mortensen, M. S.; Krogfelt, K. A.; Clegg, S. Role of *Klebsiella pneumoniae* Type 1 and Type 3 Fimbriae in Colonizing Silicone Tubes Implanted into the Bladders of Mice as a Model of Catheter-Associated Urinary Tract Infections. *Infect. Immun.* **2013**, *81*, 3009–3017.
- (12) Pratt, L.; Kolter, R. Genetic Analysis of *Escherichia coli* Biofilm Formation: Roles of Flagella, Motility, Chemotaxis and Type I Pili. *Mol. Microbiol.* **1998**, *30*, 285–293.
- (13) Rodrigues, D. F.; Elimelech, M. Role of Type 1 Fimbriae and Mannose in the Development of *Escherichia coli* K12 biofilm: from Initial Cell Adhesion to Biofilm Formation. *Biofouling* **2009**, *25*, 401–411.
- (14) Zhu, Z.; Wang, J.; Lopez, A. I.; Yu, F.; Huang, Y.; Kumar, A.; Li, S.; Zhang, L.; Cai, C. Surfaces Presenting  $\alpha$ -phenyl Mannoside Derivatives Enable Formation of Stable, High Coverage, Non-Pathogenic *Escherichia coli* Biofilms Against Pathogen Colonization. *Biomater. Sci.* **2015**, *3*, 842–851.
- (15) Rosenberg, M.; Bayer, E. A.; Delarea, J.; Rosenberg, E. Role of Thin Fimbriae in Adherence and Growth of *Acinetobacter calcoaceticus* Rag-1 on Hexadecane. *Appl. Environ. Microbiol.* **1982**, *44*, 929–937.
- (16) Kang, Z.; Yeung, A.; Foght, J. M.; Gray, M. R. Hydrophobic Bacteria at the Hexadecane–Water Interface: Examination of Micro-metre-Scale Interfacial Properties. *Colloids Surf., B* **2008**, *67*, 59–66.
- (17) Kang, Z.; Yeung, A.; Foght, J. M.; Gray, M. R. Mechanical Properties of Hexadecane–Water Interfaces with Adsorbed Hydrophobic Bacteria. *Colloids Surf., B* **2008**, *62*, 273–279.
- (18) Dorobantu, L. S.; Yeung, A. K. C.; Foght, J. M.; Gray, M. R. Stabilization of Oil-Water Emulsions by Hydrophobic Bacteria. *Appl. Environ. Microbiol.* **2004**, *70*, 6333–6336.
- (19) Abbasnezhad, H.; Gray, M.; Foght, J. M. Influence of Adhesion on Aerobic Biodegradation and Bioremediation of Liquid Hydrocarbons. *Appl. Microbiol. Biotechnol.* **2011**, *92*, 653–675.
- (20) Hermansson, M.; Kjelleberg, S.; Korhonen, T. K.; Stenström, T.-A. Hydrophobic and Electrostatic Characterization of Surface Structures of Bacteria and its Relationship to Adhesion to an Air-Water Interface. *Arch. Microbiol.* **1982**, *131*, 308–312.
- (21) Gu, H.; Chen, A.; Song, X.; Brasch, M. E.; Henderson, J. H.; Ren, D. How *Escherichia coli* Lands and Forms Cell Clusters on a Surface: A New Role of Surface Topography. *Sci. Rep.* **2016**, *6*, 29516.
- (22) Thomas, W.; Trintchina, E.; Forero, M.; Vogel, V.; Sokurenko, E. V. Bacterial Adhesion to Target Cells Enhanced by Shear Force. *Cell* **2002**, *109*, 913–923.
- (23) Nilsson, L.; Thomas, W.; Trintchina, E.; Vogel, V.; Sokurenko, E. Catch Bond-mediated Adhesion without a Shear Threshold: Trimannose Versus Monomannose Interactions with the FimH Adhesin of *Escherichia coli*. *J. Biol. Chem.* **2006**, *281*, 16656–16663.
- (24) Sharma, S.; Jaimes-Lizcano, Y. A.; McLay, R. B.; Cirino, P. C.; Conrad, J. C. Subnanometric Roughness Affects the Deposition and Mobile Adhesion of *Escherichia coli* on Silanized Glass Surfaces. *Langmuir* **2016**, *32*, 5422–5433.
- (25) Bos, R.; van der Mei, H. C.; Busscher, H. J. Physico-Chemistry of Initial Microbial Adhesive Interactions - Its Mechanisms and Methods for Study. *FEMS Microbiol. Rev.* **1999**, *23*, 179–230.
- (26) Wang, Y.; Lee, S. M.; Dykes, G. The Physicochemical Process of Bacterial Attachment to Abiotic Surfaces: Challenges for Mechanistic Studies, Predictability and the Development of Control Strategies. *Crit. Rev. Microbiol.* **2015**, *41*, 452–464.
- (27) Van Oss, C. J. The Forces Involved in Bioadhesion to Flat Surfaces and Particles — Their Determination and Relative Roles. *Biofouling* **1991**, *4*, 25–35.
- (28) Hermansson, M. The DLVO Theory in Microbial Adhesion. *Colloids Surf., B* **1999**, *14*, 105–119.
- (29) Marshall, K. C.; Stout, R.; Mitchell, R. Mechanism of the Initial Events in the Sorption of Marine Bacteria to Surfaces. *J. Gen. Microbiol.* **1971**, *68*, 337–348.
- (30) van Loosdrecht, M. C. M.; Lyklema, J.; Norde, W.; Zehnder, A. J. B. Bacterial Adhesion: A Physicochemical Approach. *Microb. Ecol.* **1989**, *17*, 1–15.
- (31) Elimelech, M. Indirect Evidence for Hydration Forces in the Deposition of Polystyrene Latex Colloids on Glass Surfaces. *J. Chem. Soc., Faraday Trans.* **1990**, *86*, 1623–1624.
- (32) Wood, J.; Sharma, R. How Long is the Long-Range Hydrophobic Attraction? *Langmuir* **1995**, *11*, 4797–4802.
- (33) Jucker, B. A.; Zehnder, A. J. B.; Harms, H. Quantification of Polymer Interactions in Bacterial Adhesion. *Environ. Sci. Technol.* **1998**, *32*, 2909–2915.
- (34) Liu, C.; Zhao, Q. Influence of Surface-Energy Components of Ni–P–TiO<sub>2</sub>–PTFE Nanocomposite Coatings on Bacterial Adhesion. *Langmuir* **2011**, *27*, 9512–9519.
- (35) Walker, S. L.; Redman, J. A.; Elimelech, M. Role of Cell Surface Lipopolysaccharides in *Escherichia coli* K12 Adhesion and Transport. *Langmuir* **2004**, *20*, 7736–7746.
- (36) Chia, T. W. R.; Nguyen, V. T.; McMeekin, T.; Fegan, N.; Dykes, G. A. Stochasticity of Bacterial Attachment and Its Predictability by the Extended Derjaguin–Landau–Verwey–Overbeek Theory. *Appl. Environ. Microbiol.* **2011**, *77*, 3757–3764.

- (37) Perni, S.; Preedy, E. C.; Prokopovich, P. Success and Failure of Colloidal Approaches in Adhesion of Microorganisms to Surfaces. *Adv. Colloid Interface Sci.* **2014**, *206*, 265–274.
- (38) Pidhatika, B.; Möller, J.; Benetti, E. M.; Konradi, R.; Rakhmatullina, E.; Mühlebach, A.; Zimmermann, R.; Werner, C.; Vogel, V.; Textor, M. The Role of the Interplay Between Polymer Architecture and Bacterial Surface Properties on the Microbial Adhesion to Polyoxazoline-Based Ultrathin Films. *Biomaterials* **2010**, *31*, 9462–9472.
- (39) Roosjen, A.; van der Mei, H. C.; Busscher, H. J.; Norde, W. Microbial Adhesion to Poly(ethylene oxide) Brushes: Influence of Polymer Chain Length and Temperature. *Langmuir* **2004**, *20*, 10949–10955.
- (40) Nejadnik, M. R.; van der Mei, H. C.; Norde, W.; Busscher, H. J. Bacterial Adhesion and Growth on a Polymer Brush-Coating. *Biomaterials* **2008**, *29*, 4117–4121.
- (41) Zhao, C.; Li, L.; Wang, Q.; Yu, Q.; Zheng, J. Effect of Film Thickness on the Antifouling Performance of Poly(hydroxy-functional methacrylates) Grafted Surfaces. *Langmuir* **2011**, *27*, 4906–4913.
- (42) Ibanescu, S.-A.; Nowakowska, J.; Khanna, N.; Landmann, R.; Klok, H.-A. Effects of Grafting Density and Film Thickness on the Adhesion of *Staphylococcus epidermidis* to Poly(2-hydroxy ethyl methacrylate) and Poly(poly(ethylene glycol)methacrylate) Brushes. *Macromol. Biosci.* **2016**, *16*, 676–685.
- (43) Taylor, R. L.; Verran, J.; Lees, G. C.; Ward, A. J. P. The Influence of Substratum Topography on Bacterial Adhesion to Polymethyl Methacrylate. *J. Mater. Sci.: Mater. Med.* **1998**, *9*, 17–22.
- (44) Hou, S.; Gu, H.; Smith, C.; Ren, D. Microtopographic Patterns Affect *Escherichia coli* Biofilm Formation on Poly(dimethylsiloxane) Surfaces. *Langmuir* **2011**, *27*, 2686–2691.
- (45) Poncin-Epaillard, F.; Herry, J. M.; Marmey, P.; Legeay, G.; Debarnot, D.; Bellon-Fontaine, M. N. Elaboration of Highly Hydrophobic Polymeric Surface — a Potential Strategy to Reduce the Adhesion of Pathogenic Bacteria? *Mater. Sci. Eng., C* **2013**, *33*, 1152–1161.
- (46) Bruinsma, G. M.; Rustema-Abbing, M.; de Vries, J.; Busscher, H. J.; van der Linden, M. L.; Hooymans, J. M. M.; van der Mei, H. C. Multiple Surface Properties of Worn RGP Lenses and Adhesion of *Pseudomonas aeruginosa*. *Biomaterials* **2003**, *24*, 1663–1670.
- (47) Truong, V. K.; Lapovok, R.; Estrin, Y. S.; Rundell, S.; Wang, J. Y.; Fluke, C. J.; Crawford, R. J.; Ivanova, E. P. The Influence of Nano-Scale Surface Roughness on Bacterial Adhesion to Ultrafine-Grained Titanium. *Biomaterials* **2010**, *31*, 3674–3683.
- (48) Etxeberria, M.; López-Jiménez, L.; Merlos, A.; Escuin, T.; Viñas, M. Bacterial Adhesion Efficiency on Implant Abutments: A Comparative Study. *Int. Microbiol.* **2013**, *16*, 235–242.
- (49) Wong, K. K. W.; Olsson, A. L. J.; Asadishad, B.; Van der Bruggen, B.; Tufenkji, N. Role of Cell Appendages in Initial Attachment and Stability of *E. coli* on Silica Monitored by Nondestructive TIRF Microscopy. *Langmuir* **2017**, *33*, 4066–4075.
- (50) Trautner, B. W.; Cevallos, M. E.; Li, H.; Riosa, S.; Hull, R. A.; Hull, S. I.; Twardy, D. J.; Darouiche, R. O. Increased Expression of Type-1 Fimbriae by Nonpathogenic *Escherichia coli* 83972 Results in an Increased Capacity for Catheter Adherence and Bacterial Interference. *J. Infect. Dis.* **2008**, *198*, 899–906.
- (51) Blattner, F. R.; Plunkett, G.; Bloch, C. A.; Perna, N. T.; Burland, V.; Riley, M.; Collado-Vides, J.; Glasner, J. D.; Rode, C. K.; Mayhew, G. F.; Gregor, J.; Davis, N. W.; Kirkpatrick, H. A.; Goeden, M. A.; Rose, D. J.; Mau, B.; Shao, Y. The Complete Genome Sequence of *Escherichia coli* K-12. *Science* **1997**, *277*, 1453–1462.
- (52) Rodrigues, D. F.; Tiedje, J. M. Multi-Locus Real-Time PCR for Quantitation of Bacteria in the Environment Reveals *Exiguobacterium* to be Prevalent in Permafrost. *FEMS Microbiol. Ecol.* **2007**, *59*, 489–499.
- (53) Livak, K.; Schmittgen, T. Analysis of Relative Gene Expression Data Using Real-Time Quantitative PCR and the  $2^{-\Delta\Delta C_T}$  method. *Methods* **2001**, *25*, 402–408.
- (54) Baker, G.; Smith, J.; Cowan, D. A. Review and Re-Analysis of Domain-Specific 16S Primers. *J. Microbiol. Methods* **2003**, *55*, 541–555.
- (55) Nagy, E.; Maier, T.; Urban, E.; Terhes, G.; Kostrzewa, M. on behalf of the Escmid Study Group on Antimicrobial Resistance in Anaerobic Bacteria. Species Identification of Clinical Isolates of *Bacteroides* by Matrix-Assisted Laser-Desorption/Ionization Time-of-Flight Mass Spectrometry. *Clin. Microbiol. Infect.* **2009**, *15*, 796–802.
- (56) Mao, S.; Zhang, R.; Wang, D.; Zhu, W. The Diversity of the Fecal Bacterial Community and its Relationship with the Concentration of Volatile Fatty Acids in the Feces During Subacute Rumen Acidosis in Dairy Cows. *BMC Vet. Res.* **2012**, *8*, 237–237.
- (57) Sokurenko, E. V.; Courtney, H. S.; Ohman, D. E.; Klemm, P.; Hasty, D. L. FimH Family of Type 1 Fimbrial Adhesins: Functional Heterogeneity due to Minor Sequence Variations among fimH Genes. *J. Bacteriol.* **1994**, *176*, 748–755.
- (58) Eshdat, Y.; Ofek, I.; Yashouv-Gan, Y.; Sharon, N.; Mirelman, D. Isolation of a Mannose-Specific Lectin From *Escherichia coli* and Its Role in the Adherence of the Bacteria to Epithelial Cells. *Biochem. Biophys. Res. Commun.* **1978**, *85*, 1551–1559.
- (59) Wu, S. Surface and Interfacial Tensions of Polymer Melts. II. Poly (methyl methacrylate), Poly (n-butyl methacrylate), and Polystyrene. *J. Phys. Chem.* **1970**, *74*, 632–638.
- (60) Niu, C.; Gilbert, E. S. Colorimetric Method for Identifying Plant Essential Oil Components That Affect Biofilm Formation and Structure. *Appl. Environ. Microbiol.* **2004**, *70*, 6951–6956.
- (61) Mejias Carpio, I. E.; Santos, C. M.; Wei, X.; Rodrigues, D. F. Toxicity of a Polymer-Graphene Oxide Composite Against Bacterial Planktonic Cells, Biofilms, and Mammalian Cells. *Nanoscale* **2012**, *4*, 4746–4756.
- (62) Fan, J.; Li, Y.; Nguyen, H. N.; Yao, Y.; Rodrigues, D. F. Toxicity of Exfoliated-MoS<sub>2</sub> and Annealed Exfoliated-MoS<sub>2</sub> Towards Planktonic Cells, Biofilms, and Mammalian Cells in the Presence of Electron Donor. *Environ. Sci.: Nano* **2015**, *2*, 370–379.
- (63) Rosenberg, M.; Gutnick, D.; Rosenberg, E. Adherence of Bacteria to Hydrocarbons: A Simple Method for Measuring Cell-Surface Hydrophobicity. *FEMS Microbiol. Lett.* **1980**, *9*, 29–33.
- (64) Ong, Y.-L.; Razatos, A.; Georgiou, G.; Sharma, M. M. Adhesion Forces between *E. coli* Bacteria and Biomaterial Surfaces. *Langmuir* **1999**, *15*, 2719–2725.
- (65) Sharma, S.; Conrad, J. C. Attachment from Flow of *Escherichia coli* Bacteria onto Silanized Glass Substrates. *Langmuir* **2014**, *30*, 11147–11155.
- (66) Zoueki, C. W.; Tufenkji, N.; Ghoshal, S. A Modified Microbial Adhesion to Hydrocarbons Assay to Account for the Presence of Hydrocarbon Droplets. *J. Colloid Interface Sci.* **2010**, *344*, 492–496.
- (67) Chang, C. B.; Wilking, J. N.; Kim, S.-H.; Shum, H. C.; Weitz, D. A. Monodisperse Emulsion Drop Microenvironments for Bacterial Biofilm Growth. *Small* **2015**, *11*, 3954–3961.
- (68) Vaccari, L.; Allan, D. B.; Sharifi-Mood, N.; Singh, A. R.; Leheny, R. L.; Stebe, K. J. Films of Bacteria at Interfaces: Three Stages of Behaviour. *Soft Matter* **2015**, *11*, 6062–6074.
- (69) Blumer, C.; Kleefeld, A.; Lehnen, D.; Heintz, M.; Dobrindt, U.; Nagy, G.; Michaelis, K.; Emödy, L.; Polen, T.; Rachel, R.; Wendisch, V. F.; Uden, G. Regulation of Type 1 Fimbriae Synthesis and Biofilm Formation by the Transcriptional Regulator LrhA of *Escherichia coli*. *Microbiology* **2005**, *151*, 3287–3298.
- (70) Worton, D. R.; Zhang, H.; Isaacman-VanWertz, G.; Chan, A. W. H.; Wilson, K. R.; Goldstein, A. H. Comprehensive Chemical Characterization of Hydrocarbons in NIST Standard Reference Material 2779 Gulf of Mexico Crude. *Environ. Sci. Technol.* **2015**, *49*, 13130–13138.
- (71) Burruss, R. C.; Ryder, R. T. *Composition of Crude Oil and Natural Gas Produced from 14 Wells in the Lower Silurian "Clinton" Sandstone and Medina Group, Northeastern Ohio and Northwestern Pennsylvania*; Open-File Report 2003–4092003.
- (72) Gonzalez, E. A.; Blanco, J.; Baloda, S. B.; Wadström, T. Relative cell surface hydrophobicity of *Escherichia coli* strains with various

recognized fimbrial antigens and without recognized fimbriae. *Zentralbl. Bakteriol., Mikrobiol. Hyg., Ser. A* **1988**, *269*, 218–236.

(73) Tokuda, H.; Matsuyama, S. Sorting of lipoproteins to the outer membrane in *E. coli*. *Biochim. Biophys. Acta, Mol. Cell Res.* **2004**, *1693*, 5–13.

(74) Heinrichs, D. E.; Yethon, J. A.; Whitfield, C. Molecular basis for structural diversity in the core regions of the lipopolysaccharides of *Escherichia coli* and *Salmonella enterica*. *Mol. Microbiol.* **1998**, *30*, 221–232.

(75) Frirdich, E.; Whitfield, C. Lipopolysaccharide inner core oligosaccharide structure and outer membrane stability in human pathogens belonging to the Enterobacteriaceae. *J. Endotoxin Res.* **2005**, *11*, 133–144.

(76) Brauner, A.; Katouli, M.; Tullus, K.; Jacobson, S. H. Cell Surface Hydrophobicity, Adherence to HeLa Cell Cultures and Haemagglutination Pattern of Pyelonephritogenic *Escherichia coli* Strains. *Epidemiol. Infect.* **1990**, *105*, 255–263.

(77) Zhang, Z.; Christopher, G. F. Effect of Particulate Contaminants on the Development of Biofilms at Air/Water Interfaces. *Langmuir* **2016**, *32*, 2724–2730.

(78) Gabr, R. M.; Gad-Elrab, S. M. F.; Abskharon, R. N. N.; Hassan, S. H. A.; Shoreit, A. A. M. Biosorption of Hexavalent Chromium Using Biofilm of *E. coli* Supported on Granulated Activated Carbon. *World J. Microbiol. Biotechnol.* **2009**, *25*, 1695–1703.

(79) Quintelas, C.; Rocha, Z.; Silva, B.; Fonseca, B.; Figueiredo, H.; Tavares, T. Removal of Cd(II), Cr(VI), Fe(III) and Ni(II) from Aqueous Solutions by an *E. coli* Biofilm Supported on Kaolin. *Chem. Eng. J.* **2009**, *149*, 319–324.

(80) Ni, L.; Yang, S.; Zhang, R.; Jin, Z.; Chen, H.; Conrad, J. C.; Jin, F. Bacteria Differently Deploy Type-IV Pili on Surfaces to Adapt to Nutrient Availability. *NPJ. Biofilms Microbiomes* **2016**, *2*, 15029.

(81) Vigeant, M. A.-S.; Wagner, M.; Tamm, L. K.; Ford, R. M. Nanometer Distances Between Swimming Bacteria and Surfaces Measured by Total Internal Reflection Aqueous Fluorescence Microscopy. *Langmuir* **2001**, *17*, 2235–2242.

(82) Vigeant, M. A.-S.; Ford, R. M.; Wagner, M.; Tamm, L. K. Reversible and Irreversible Adhesion of Motile *Escherichia coli* Cells Analyzed by Total Internal Reflection Aqueous Fluorescence Microscopy. *Appl. Environ. Microbiol.* **2002**, *68*, 2794–2801.

(83) Molaei, M.; Barry, M.; Stocker, R.; Sheng, J. Failed Escape: Solid Surfaces Prevent Tumbling of *Escherichia coli*. *Phys. Rev. Lett.* **2014**, *113*, 068103.

(84) Qi, M.; Gong, X.; Wu, B.; Zhang, G. Landing Dynamics of Swimming Bacteria on a Polymeric Surface: Effect of Surface Properties. *Langmuir* **2017**, *33*, 3525–3533.

(85) Wang, H.; Wilksch, J. J.; Chen, L.; Tan, J. W. H.; Strugnell, R. A.; Gee, M. L. Influence of Fimbriae on Bacterial Adhesion and Viscoelasticity and Correlations of the Two Properties with Biofilm Formation. *Langmuir* **2017**, *33*, 100–106.